Bulletin of Mathematical Biology (2021) 83:24
https://doi.org/10.1007/s11538-020-00846-4

Society for Mathematical Biology

ORIGINAL ARTICLE

Stochastic Chlamydia Dynamics and Optimal Spread

German Enciso[1] · Christine Sütterlin[2] · Ming Tan[3] · Frederic Y. M. Wan[1]

Received: 6 May 2020 / Accepted: 9 December 2020 / Published online: 17 February 2021

Abstract
Chlamydia trachomatis is an important bacterial pathogen that has an unusual developmental switch from a dividing form (reticulate body or RB) to an infectious form (elementary body or EB). RBs replicate by binary fission within an infected host cell, but there is a delay before RBs convert into EBs for spread to a new host cell. We developed stochastic optimal control models of the Chlamydia developmental cycle to examine factors that control the number of EBs produced. These factors included the probability and timing of conversion, and the duration of the developmental cycle before the host cell lyses. Our mathematical analysis shows that the observed delay in RB-to-EB conversion is important for maximizing EB production by the end of the intracellular infection.

Keywords Chlamydia · Infectious disease · Birth and death processes · Optimal control · Stochastic optimization

Mathematics Subject Classification Primary 60H10 · 49J15; Secondary 93E20 · 92B05

1 Introduction

1.1 *Chlamydia trachomatis* and Its Development Cycle

Chlamydia trachomatis is a major cause of genital and eye infections in humans (Batteiger and Tan 2019). There were an estimated 131 million new cases of *C. trachomatis*

The research is partially supported by NSF (UBM) Grant DMS-1129008 for the UCI MCBU Program. MCBU students did some computing related to this research but is not used in this report.

✉ German Enciso
enciso@uci.edu

1 Department of Mathematics, University of California Irvine, Irvine, USA

2 Department of Developmental and Cell Biology, University of California Irvine, Irvine, USA

3 Department of Microbiology and Molecular Genetics, University of California Irvine, Irvine, USA

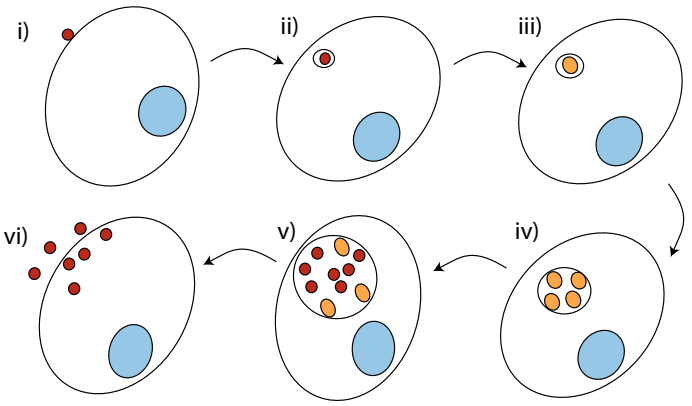

Fig. 1 (*i*) The elementary body (EB) binds the host cell and (*ii*) enters within a membrane-bound compartment called the chlamydial inclusion. (*iii*) The EB converts into a replicating form called the reticulate body (RB), (*iv*) which divides repeatedly by binary fission. (*v*) About halfway through the 48-h intracellular infection, RBs begin to convert into EBs in an asynchronous manner. (*vi*) The developmental cycle ends when the host cell lyses and EBs are released to infect new host cells. RBs that have not yet converted are not infectious. Figure from Wan and Enciso (2017) (Color figure online)

genital infection in 2012, making it the most common cause of sexually transmitted bacterial infection (Newman 2015). This pathogen also causes trachoma, which is the world's leading cause of preventable blindness. 21 million people are estimated to have active trachoma (Taylor et al. 2014) of which 1.9 million individuals are blind or have severe visual impairment (World Health Organization 2020). Trachoma has been targeted for elimination by the World Health Organization.

C. trachomatis replicates by means of an unusual 2-day developmental cycle that takes place within a human, or other eukaryotic, host cell (Fig. 1) (Abdelrahman and Belland 2005; Lee et al. 2018; Moulder 1991). Unlike most bacteria, Chlamydia exists in two distinct morphological forms, each with a specialized function. The infectious form, called an elementary body (EB), binds and enters a host cell. However, the EB cannot divide and instead converts into a reticulate body (RB), which is the replicating form of the bacterium. Within a membrane-bound compartment known as the chlamydial inclusion, the RB divides repeatedly by binary fission, which expands the RB population. Then after a period of no conversion (a conversion holiday), individual RBs each convert into an EB. This conversion event occurs asynchronously, so that some RBs are converting into EBs, while others continue to divide. Thus, at late times in the intracellular infection, the inclusion contains a mixture of RBs, EBs, dividing RBs, and intermediate bodies (IBs), which are RBs in the process of converting into EBs. This mix of chlamydial forms is released into the extracellular space when the host cell lyses. RB-to-EB conversion is a critical step in the developmental cycle because RBs are not infectious, and only EBs can spread the infection to a new host cell.

Until recently, these developmental events of the intracellular Chlamydia infection had not been quantified. Conventional electron microscopy of a Chlamydia-infected cell analyzes a section through the inclusion, and thus reveals the relative pro-

portions, but not accurate numbers, for each developmental form Belland (2003), Hackstadt et al. (1997) and Shaw (2000). Using a novel three-dimensional electron microscopy approach known as serial block-face scanning electron microscopy (Denk and Horstmann 2004; Leighton 1981), the labs of Tan and Sütterlin recently performed a comprehensive analysis of the chlamydial inclusion. This study quantified the changing number of RBs and EBs in the inclusion over the course of the developmental cycle (Lee et al. 2018). This analysis also provided extensive quantitative data on RB replication and RB-to-EB conversion because it was able to identify and quantify RBs undergoing replication (dividing RBs; referred to as DBs in this study) or conversion (IBs).

This study confirmed the delayed and asynchronous nature of RB-to-EB conversion, and also measured a 6-fold decrease in average RB size as the RB population expanded. Taking into account the correlation between small RB size and the onset of RB-to-EB conversion, Lee et al. proposed a size control mechanism in which RBs reduce in size through replication, and cannot convert into an EB until they are below a size threshold (Lee et al. 2018). They also showed that a mathematical model based on this size control mechanism, and utilizing measured and calculated parameter values and Gamma distributions, replicated growth curves for the developmental cycle.

In the current report, we have used the extensive data from the Lee et al. study to conduct a theoretical investigation of the Chlamydia developmental cycle. This analysis reveals that the dynamics of the developmental cycle, with delayed conversion from RBs to EBs, is a successful strategy for the bacterium to maximize the production of infectious progeny and, thus, the spread of the intracellular infection to a new host cell.

1.2 Maximum Spread of Infection and Selective Pressure

With a high RB-to-EB conversion rate (relative to RB proliferation rate), allowing more RBs to divide at an early stage would generate more RBs for later conversion to more infectious EBs to be discharged when the host cell lyses. With its initial conversion holiday, the Chlamydia development cycle would increase the terminal EB population for a larger spread of the bacterial infection. In a Darwinian world of natural selection, maximizing terminal EB strategy would be seen as the bacterial response to the pressure of competitive species survival.

To assess the validity of this posit, a two-form deterministic model (the PT-Model) that captures the essential features of the developmental cycle for the RB and EB populations was formulated and analyzed in Wan and Enciso (2017) for a particular chlamydial inclusion. With the (per unit RB) conversion rate $u(t)$ as the control, the model seeks the optimal $u(t)$ that maximizes the EB population at the terminal time T when the host cell lyses. For the biologically relevant conversion capacity range, optimal maximizing strategy of this PT-Model does in fact start with a conversion holiday. The small size threshold for conversion eligibility, not stipulated in the model, is seen as an instrument for inducing this initial period of no conversion.

In reality, the lysis time of an infected cell varies, but has not been quantified empirically. Data collected in Lee et al. (2018) and elsewhere also show variability of

in other developmental features. Probabilistic models would be needed to address the observed stochasticity. Two such models (the WS-Model of Sect. 3 and the RT-Model of Sect. 4), are formulated and analyzed in this paper for this purpose. Both are based on a birth and death process model (the BD-Model) of Sect. 2. The optimal strategy for maximizing the mean terminal EB population will be shown to also require a conversion holiday at the start, again supporting our posit for this case of infected cells embedded in an uncertain environment. As in the PT-Model of Wan and Enciso (2017), there is no stipulated enabling mechanism such as a size-threshold requirement for conversion eligibility to dictate an initial period of no conversion in the optimal maximizing strategy; rather, the conversion holiday in the development cycle generated by the WS-Model and the RT-Model are natural consequences of maximizing the terminal (mean) EB population.

1.3 Post Conversion Holiday RB Growth

To keep the modeling and analysis manageable, the four relevant (PT-, BD-, WS- and RT-) models are for two (lumped) forms (RB and EB) of the Chlamydia population (unlike the four-form GD-Model for RB, DB, IB and EB in Lee et al. 2018). Without multiple divisions to reach the conversion eligibility threshold size, these two-form models are not sufficiently fine-grained for matching the reported data beyond the conversion holiday phase of the bacterial growth. (For that reason, no attempt will be made to validate our models by comparing numerical solution with available data herein.) Quite the contrary, we note in Sect. 6 a qualitative difference between predictions by our two form optimal control models and the available data after the initiation of RB-to-EB conversion. More specifically, data collected in Lee et al. (2018) show a continual growth of the RB population after the initiation of RB-to-EB conversion at least for a period. In contrast, the three (PT-, WS- and RT-) models show an immediate and continual decline of the expected RB population after the onset of RB-to-EB conversion. We conclude this paper by a brief description of how this deficiency is remedied by a four-form model (designated as the *MP-Model*).

1.4 A Summary of Relevant Models

For clarity, a brief description of the relevant models discussed herein can be found in "Appendix A".

2 A Birth and Death Process Model (*The BD-Model*)

2.1 The Kolmogorov Equations

We begin by modeling RB proliferation (birth) and RB-to-EB conversion (death) of the *Chlamydia* developmental cycle as a birth and death process to capture the basic activities for the bacteria to proliferate and spread infection . Denote by R_t and E_t the random variable for the size of *RB* and *EB* population, respectively, at time t. Let

$P_k(t)$ and $Q_j(t)$ be the probability of R_t and E_t be of size k and j, respectively, at time t. With assumptions similar to those for various birth and death models (such as stationarity, independent increments and a sufficiently short elapsed time δt for no more than one division or conversion), we have the following relations for $P_k(t+\delta t)$ and $Q_j(t+\delta t)$:

$$P_k(t+\delta t) = \{1 - k(\lambda_D + \lambda_C)\delta t\}\, P_k(t) + (k+1)\lambda_C \delta t\, P_{k+1}(t) + (k-1)\lambda_D \delta t\, P_{k-1}(t)$$

and

$$\begin{aligned} Q_j(t+\delta t) = {} & \{1 - \lambda_C \delta t\, P_1(t) - 2\lambda_C \delta t\, P_2(t) - 3\lambda_C \delta t\, P_3(t) - \cdots\}\, Q_j(t) \\ & + \lambda_C \delta t\, \{P_1(t) + 2P_2(t) + 3P_3(t) + \cdots\}\, Q_{j-1}(t) \end{aligned}$$

except for negligibly small terms relative to terms proportional to δt. In these two relations, $\lambda_C \delta t$ and $\lambda_D \delta t$ are the probability of one conversion and one duplication, respectively, during the elapsed time δt. Since our experimental findings clearly show a time varying RB-to-EB conversion rate (Lee et al. 2018), the present linear birth and death model (the *BD-Model*) henceforth works with a time varying $\lambda_C(t)$ but keep λ_D constant since there is no indication to suggest otherwise.

This system of interactions approximately corresponds to the reactions $R \longrightarrow 2R$, $R \longrightarrow E$ with rates λ_D, λ_C respectively, using notation for chemical reactions. We use separate variables for the states P_k and Q_j rather than a joint state for RBs and EBs, in order to carry out the analysis in the next section.

In the limit as δt tends to zero, we get the following ODE systems

$$\frac{\mathrm{d}P_k}{\mathrm{d}t} = -k(\lambda_D + \lambda_C)P_k + (k+1)\lambda_C P_{k+1} + (k-1)\lambda_D P_{k-1}, \tag{1}$$

$$\frac{\mathrm{d}Q_j}{\mathrm{d}t} = \lambda_C \left(Q_{j-1} - Q_j\right) \sum_{i=0}^{\infty} i\, P_i, \tag{2}$$

augmented by the initial conditions $P_k(0) = \delta_{kN}$ and $Q_j(0) = 0,\ k, j = 0, 1, 2, \ldots$, given that the process starts with N RB units and no EB.

2.2 Solution by Generating Functions

The ODE system for $P_k(t)$ and $Q_j(t)$ can be reformulated as a problem for the corresponding probability generating functions (pgf)

$$G(x,\tau) = \sum_{k=0}^{\infty} P_k(t) x^k, \qquad F(x,\tau) = \sum_{k=0}^{\infty} Q_k(t) x^k. \tag{3}$$

with $G(x,\tau)$ and $F(x,\tau)$ determined by

$$\frac{\partial G}{\partial \tau} + \left\{(1+\rho)x - \rho - x^2\right\} \frac{\partial G}{\partial x} = 0 \tag{4}$$

and

$$\frac{\partial F}{\partial \tau} + \rho(1-x)\bar{R}_t F = 0 \tag{5}$$

with

$$\tau = \lambda_D t, \qquad \rho(\tau) = \frac{\lambda_C(t)}{\lambda_D}, \qquad \bar{R}_t(\tau) = \sum_{k=0}^{\infty} k P_k(t) \tag{6}$$

The initial conditions for $\{P_k(t)\}$ and $\{Q_j(t)\}$ require

$$G(x,0) = x^N, \qquad F(x,0) = 1. \tag{7}$$

The solution for $G(x,\tau)$ is found by the method of characteristics in "Appendix B" to be

$$G(x,\tau) = x_0^N = \left\{1 + \frac{x-1}{e^{f(\tau)} - (x-1)I(\tau)}\right\}^N \tag{8}$$

where

$$f(\tau) = -\tau + \int_0^\tau \rho(\xi)\mathrm{d}\xi, \qquad I(\tau) = \int_0^\tau e^{f(\zeta)}\mathrm{d}\zeta. \tag{9}$$

Unlike the PDE (4) for the generating function $G(x,\tau)$ of the sequence $\{P_k(\tau)\}$, the corresponding equation (5) for the generating function $F(x,\tau)$ of the sequence $\{Q_k(\tau)\}$ is effectively an ODE that is separable in time with x as a parameter. With $\bar{R}_t(\tau)$ given by (11), Eq. (5) for $F(x,\tau)$ becomes

$$\frac{\mathrm{d}F}{\mathrm{d}\tau} = (x-1)\rho(\tau)\bar{R}_t(\tau)F = (x-1)\rho(\tau)Ne^{-f(\tau)}F$$

so that

$$F(x,\tau) = e^{N(x-1)\int_0^\tau \rho(\zeta)e^{-f(\zeta)}\mathrm{d}\zeta} \tag{10}$$

with $F(x,0) = 1$ meeting the condition of no EB initially.

2.3 Means and Variances

2.3.1 Expected RB Population

The expected RB population as a function of time is then given by

$$\begin{aligned}\bar{R}_t(\tau) \equiv E[R_t] &= \sum_{k=0}^{\infty} k P_k(t) = \left[\frac{\partial G}{\partial x}\right]_{x=1} \\ &= \left[\frac{N x_0^{N-1} e^{f(\tau)}}{\left\{e^{f(\tau)} - (x-1)I(\tau)\right\}^2}\right]_{x=1} = Ne^{-f(\tau)}\end{aligned} \tag{11}$$

A differential form of the solution for $\bar{R}_t(\tau)$, needed in subsequent development, is obtained by differentiating both sides of (11) to get

$$\frac{\mathrm{d}\bar{R}_t}{\mathrm{d}\tau} = Ne^{-f(\tau)}\left\{-\frac{\mathrm{d}f}{\mathrm{d}\tau}\right\} = (1-\rho)\,\bar{R}_t, \qquad \bar{R}_t(0) = N. \tag{12}$$

For the special case of a constant conversion probability λ_C so that ρ is a constant, the mean populations (11) and (15) simplify to

$$\bar{R}_t(\tau;\rho) \equiv E[R_t] = \sum_{k=0}^{\infty} k P_k(t) = Ne^{(1-\rho)\tau} \tag{13}$$

with

$$\bar{R}_t(\tau;1) \equiv E[R_t] = N \tag{14}$$

for the special case $\lambda_C = \lambda_D$. For $\lambda_C \neq \lambda_D$, we have the following limiting behavior for the mean RB population:

$$\lim_{t\to\infty}\left[\bar{R}_t(\tau;\rho)\right] = \begin{cases} 0 & (\lambda_D < \lambda_C) \\ \infty & (\lambda_D > \lambda_C) \end{cases}.$$

(The expressions $E[R_t]$ and $\bar{R}_t(\tau;\rho)$ will be used interchangeably for the expected RB population size as a function of time t with $\tau = \lambda_D t$ and $\rho = \lambda_C/\lambda_D$.)

2.3.2 Expected EB Population

The expected EB population at any instant in time is then

$$\bar{E}_t(\tau) \equiv E[E_t] = \left[\frac{\partial F}{\partial x}\right]_{x=1} = N\int_0^{\tau} \rho(\zeta)e^{-f(\zeta)}\mathrm{d}\zeta. \qquad (\tau = \lambda_D t) \tag{15}$$

We will also need the following differentiated form of this result obtained by differentiating (15) with respect to τ to get

$$\frac{\mathrm{d}\bar{E}_t}{\mathrm{d}\tau} = N\rho(\tau)e^{-f(\tau)} = \rho\bar{R}_t, \qquad \bar{E}_t(0) = 0. \tag{16}$$

The expected EB population for a constant ρ is

$$\bar{E}_t(\tau;\rho) \equiv E[E_t] = \sum_{k=0}^{\infty} k Q_k(t) = \frac{\rho N}{1-\rho}\left[e^{(1-\rho)\tau} - 1\right] \qquad (\rho \neq 1) \tag{17}$$

and, as a limiting case of (17) as $\rho \to 1$,

$$\bar{E}_t(\tau;1) = N\tau. \tag{18}$$

Note that we have

$$\lim_{t \to \infty} \left[\bar{E}_t(\tau; \rho)\right] = \infty$$

for all $\rho > 0$.

2.3.3 Variance of EB Population

For the corresponding variances, we note

$$\left[\frac{\partial^2 F}{\partial x^2}\right]_{x=1} = \left[\sum_{k=0}^{\infty} k(k-1) Q_k x^{k-2}\right]_{x=1} = E[E_t^2] - E[E_t]$$

so that

$$Var\,[E_t] = E[E_t^2] - (E[E_t])^2 = \left[\frac{\partial^2 F}{\partial x^2}\right]_{x=1} + E[E_t] - (E[E_t])^2.$$

But we have from (10)

$$\left[\frac{\partial^2 F}{\partial x^2}\right]_{x=1} = \left(N \int_0^{\tau} \rho(\zeta) e^{-f(\zeta)} \mathrm{d}\zeta\right)^2 = (E[E_t])^2$$

so that

$$Var\,[E_t] = E[E_t].$$

Proposition 1 *For our BD-Model, the variance of the EB population is the same as the mean population.*

Remark 1 From the partial derivative of the pgf $F(x, \tau)$ in x, it is seen that the distribution of E_t may be written as

$$Q_k(\tau) = \frac{z^k(\tau)}{k!} e^{-z(\tau)}, \qquad z(\tau) = N \int_0^{\tau} \rho(\zeta) e^{-f(\zeta)} \mathrm{d}\zeta$$

so that the EB process is Poisson in $z(\tau)$.

2.3.4 Variance of RB Population

For the RB population, we have similarly

$$Var[R_t] = \left[\frac{\partial^2 G}{\partial x^2}\right]_{x=1} + E[R_t] - (E[R_t])^2$$

with

$$E[R_t] = \left[\frac{\partial G}{\partial x}\right]_{x=1} = N e^{-f(\tau)}$$

by (11). From (8), we have

$$\left[\frac{\partial^2 G}{\partial x^2}\right]_{x=1} = \frac{1}{N}\left(E[R_t]\right)^2\{N-1+2I\}$$

so that

$$Var[R_t] = E[R_t]\left\{\frac{N-1+2I}{N}\right\} \tag{19}$$

For a constant $\rho \neq 1$, we have from (9)

$$Var[R_t] = \frac{1+\rho}{1-\rho}\left(e^{(1-\rho)\tau}-1\right)E[R_t].$$

Note that the variance of the RB process is generally not equal to the mean of the process.

3 Maximum Expected EB Population at Host Cell Lysis Time (*The WS-Model*)

3.1 Terminal Time of Life Cycle

While the *BD-Model* captures the basic RB activities to proliferate and convert to EB during the chlamydial developmental cycle, such activities are known to terminate in finite time. Unless the host cell lyses at some instant T so that the EB units are released to infect other hosts, the bacteria would not be able to spread and thereby risk eventual extinction. Experimental findings show the finite lysis times of different host cells span over a significantly large time interval and cannot be approximated by a single numerical value. The majority of *C. trachomatis*-infected cells among the data collected lyse between 48 and 72 h post infection (hpi), see Elwell et al. (2016); Hybiske and Stephens (2007). Yet these and other available data do not offer a definitive guide or directive toward the cause or process that induce lysing. To amplify, data collected in Lee et al. (2018) shows that the total Chlamydia units in a cytoplasmic inclusion typically tend to an upper limit after 32 hpi. The inclusion volume also increases with time at the early stage of the developmental cycle but also ceases to increase near the end. It was found that the total volume (size) of the chlamydiae actually reduces while the total number of bacterial units increases; yet available space for more chlamydiae does not appear to be an issue.

Absent of sufficient information for the determination of the host cell lysis time, a plausible criterion for Chlamydia developmental cycle termination is formulated here to illustrate one approach to complete the specification of the optimization problem that reflects the bacteria's expected response to the pressure of natural selection. Given the limited capacity of the inclusion that houses the Chlamydia units within the host cell, the approach adopted here would have the host cell lysing at the instant T when a weighted sum of the *expected* RB and EB population, $\bar{R}_t$ and $\bar{E}_t$, reaches a threshold

size P_c (not necessarily in excess of the inclusion's capacity)

$$\left\{n\bar{E}_t(\tau;\rho) + m\,\bar{R}_t(\tau;\rho)\right\}_{t=T} \equiv n\,\bar{E}_T + m\,\bar{R}_T = P_c. \tag{20}$$

(leading to the name WS-Model) for $n > 0$ while m may be of either sign to be explained below. Given the stochastic nature of proliferation and conversion process in the BD-Model, the criterion (20) allows for variations of T among the different host cells.

The condition (20) with $m > 1$ may be associated with the relative size of the EB and RB particles (by a factor of 50 at the start and down to about 5 near the end). Experimental findings reported in Lee et al. (2018) also suggest that there are additional factors contributing to the host cell lysis. Among these is EB particles secreting chemicals that enhance host cell lysing. This effect may capture by a suitably large positive n in (20). Depending on the potency of the lysis inducing EB chemicals, the ratio $m/n > 0$ may be > 1 or < 1.

Observations in Lee et al. (2018) also suggest the possibility of RB particles exhibiting inhibitory effects on host cell lysing to prolong their own existence. In the context of the threshold condition (20), such inhibitory effects may be incorporated by modifying it to read

$$n\,\bar{E}_T + (m-i)\,\bar{R}_T = P_c, \tag{21}$$

for some parameter $i > 0$ characterizing the inhibitory effects of the RB population. Equation (21) is again of the form (20) with $m - i$ taking the place of m. Given $n \geq 1$, we may divide the threshold condition (20) above through by n and write the result as

$$\bar{E}_T + m_{\,c}\bar{R}_T = P_c, \tag{22}$$

where $m_c = (m-i)/n$ may be > 1, < 1 or < 0.

Before adopting this condition for the optimization of the expected terminal EB population, we note briefly the situation for the special case where the conversion probability does not vary with time. In that case, the optimal conversion probability is $\lambda_C^* = \lambda_D$ (or $\rho = 1$) and then it is a calculus problem to obtain as the maximum expected EB

$$\left(\bar{E}_T\right)_{\max} = (P_c - m_c N)\,, \tag{23}$$

to be attained at the terminal time

$$T_{\max} = \frac{P_c - m_c N}{\lambda_D N}. \tag{24}$$

where m_c may be negative or positive. We see from (24) and (23) that the terminal time would be later for $m_c > 1$ with a larger expected terminal EB population. (Data reported in Lee et al. (2018) suggest that m_c may change with time but the condition (20) involves on m_c at the terminal time so the temporal variation of m_c is not relevant for the WS-Model.)

Remark 2 The following two observations are appropriate at this time:

- The requirement of optimal conversion probability $\lambda_C^* = \lambda_D$ ($\rho^* = 1$) may not be met if the conversion capacity is limited so that λ_C is restricted to be $\lambda_C^* \le \lambda_{\max} < \lambda_D$. For $\lambda_{\max} < \lambda_D$, we should presumably convert (suboptimally) at $\lambda_C^* = \lambda_{\max}$.
- Experimental data reported in Lee et al. (2018) suggest a terminal time T of about 42–48 hpi. On the other hand, the theoretical optimal time $T_{\max}$ to maximum expected terminal EB population for $\lambda_C^* = \lambda_D$ as given by (24) is about 5,000 hpi way to long to be biologically realistic.

3.2 An Optimal Control Formulation

To find the $\rho(\tau)$ that maximizes the expected EB population at some terminal time T, denoted by $\bar{E}_T \equiv \bar{E}_t(\tau_T)$ with $\tau_T = \lambda_D T$, it is well-known that the appropriate method of solution for this type of problems is the method of optimal control. For this reason, we henceforth change to the more conventional optimal control notations, writing $u(t)$, α, E_T, $E(t)$ and $R(t)$ for $\lambda_C(t)$, λ_D, $\bar{E}_T$, $\bar{E}_t(\tau)$ and $\bar{R}_t(\tau)$, respectively. There is also the additional benefit of being able to compare directly with the results for the deterministic optimal control problems of Wan and Enciso (2017) and Wan (2018). In terms of the optimal control notations, the results for the expected RB and EB populations, $R(t) \equiv \bar{R}_t(\tau)$ and $E(t) \equiv \bar{E}_t(\tau)$, associated with the BD Model of the last section are restated in differential form below to be referenced in the ensuing optimal control analysis:

Proposition 2 *The rates of growth of the expected RB population $R(t) \equiv \bar{R}_t(\tau)$ and the expected EB population $E(t) \equiv \bar{E}_t(\tau)$ in physical time t are determined by the two IVP*

$$R' = (\alpha - u)R, \quad R(0) = N, \tag{25}$$

$$E' = uR, \quad E(0) = 0, \tag{26}$$

respectively, with $(\ )' = d(\ )/dt$.

With $\rho = \lambda_C(t)/\lambda_D = u(t)/\alpha$, the IVP (25) and (26) are merely (12) and (16), respectively, in the new notations. For $R(t)$ and $E(t)$ to be differentiable, we limit admissible $u(t)$ ($\equiv \lambda_C(t)$) to the set Ω of *piecewise smooth* (PWS) functions. In terms of un-normalized quantities $R(t)$ and $E(t)$, our optimization problem as

$$\max_{u \in \Omega} [\, E_T = \int_0^T uR\mathrm{d}t \,], \tag{27}$$

subject to the growth dynamics and initial condition (25) for $R(t)$ and the terminal constraint

$$E(T) + m_c\, R(T) = P_c, \tag{28}$$

with $R_T = R(T)$ being the (expected) terminal RB population in the new notation.

Given the reality of a limit to the capacity to convert, there is an upper bound on the one-way RB-to-EB conversion. The optimal choice $u_{op}(t)$ among all $u(t)$ in the

admissible set Ω is required to satisfy the inequality constraints

$$0 \leq u(t) \leq u_{\max}. \tag{29}$$

3.3 The Maximum Principle

The appropriate method for finding the optimal conversion rate $u_{op}(t)$ that maximizes the expected terminal EB population E_T is the Maximum Principle (Bryson and Ho 1969; Wan 1995; Pontryagin 1962). For this method of solution, we introduce the Hamiltonian

$$H[u] \equiv H(R, E, \lambda, u) = \lambda(\alpha - u)R + uR = \lambda\alpha R + (1 - \lambda)uR \tag{30}$$

and form the following adjoint differential equation

$$\frac{\mathrm{d}\lambda}{\mathrm{d}t} = -\frac{\partial H}{\partial R} = -\lambda(\alpha - u) - u \tag{31}$$

to be satisfied by an adjoint function (aka Lagrange multiplier) $\lambda(t)$ as a necessary condition required by the Maximum Principle. The adjoint DE (31) and the growth dynamics DE in (25) constitute a Hamiltonian system supplemented by only one auxiliary condition in (25) on the unknown $R(t)$ prescribed at $t = 0$ of the solution domain $[0, T]$. The Maximum Principle then requires the adjoint function $\lambda(t)$ to satisfied the adjoint (Euler) boundary condition

$$\lambda(T) = 0. \tag{32}$$

If the control $u(t)$ should have a finite jump discontinuity at an instant t_s in $(0, T)$, the Maximum Principle requires that the Hamiltonian be continuous at the *switch point* t_s:

$$[H]_{t=t_s-}^{t_s+} = 0. \tag{33}$$

Finally, the *optimal control* $u_{op}(t)$ must maximize $H(t)$ in the sense

$$[H]_{u=u_{op}(t)} = \max_{u \,\epsilon\, \Omega} \left[H(R^*, E^*, \lambda^*, u)\right] = H(R^*, E^*, \lambda^*, u_{op}(t)) \tag{34}$$

where $(\,)^*$ is the quantity $(\,)$ induced by the optimal control. As we shall see, this last step constitutes the most challenging part of the solution process for our problem.

The second order ODE system (25) and (31) is supplemented by two auxiliary conditions: the initial condition in (25) and the Euler boundary condition (32). Together, they determine the state function $R(t)$ and adjoint function $\lambda(t)$, with the terminal time T determined by the threshold condition (28) once we know the control $u(t)$. If the control should have a finite jump discontinuity at a switch point t_s, the switch condition (33) applies to determine the switch point.

In principle, the optimal control $u_{op}(t)$ is specified by the stationary condition (34) to complete the solution process. From the requirements imposed by the Maximum

Principle, we readily observe in the following three sections three key results pertaining to the optimal conversion strategy, i.e., the *optimal control* $u_{op}(t)$.

3.4 Singular Solution Not Applicable

Suppose we have the state and adjoint functions corresponding to the optimal control $u_{op}(t)$. Then the dependence of the Hamiltonian on the control must be such that $u_{op}(t)$ is one of its maximum points. We should therefore seek $u_{op}(t)$ among the stationary points $u_S(t)$ of the Hamiltonian $H[u(t)]$. Since H is differentiable with respect to u, we use (34) in the form

$$\frac{\partial H}{\partial u} = R(-\lambda + 1) = 0. \tag{35}$$

to determine an interior extremum. Now, the relation (35) does not involve the control $u(t)$ and therefore does not provide any clue to $u_S(t)$ directly. But with $R(t) > 0$, an interior extremum would require the adjoint function to be the *singular solution*

$$\lambda^{(s)}(t) = 1. \tag{36}$$

In principle, the singular solution (36) being an interior extremum should be preferred. However, it is not applicable in any sub-interval of the solution domain. Given

$$0 = \frac{\mathrm{d}\lambda^{(s)}}{\mathrm{d}t} = -\lambda^{(s)}(\alpha - u) - u = -\alpha < 0,$$

being an impossibility, the singular solution does not satisfy the necessary condition (31) required by the Maximum Principle in any sub-interval (t_1, t_2) of the solution domain. Hence, it is not a part of the solution for the problem. We have thus established the following negative result for our problem:

Proposition 3 *The singular solution* (36) *has no role in the solution for our maximum (mean) terminal EB population problem defined by* (27), (25), (28) *and* (29) *with a time-varying control.*

3.5 Optimal Conversion Rate

We limit discussion only to the biologically realistic case of $u_{\max} > \alpha$ (see Figure 5G of Lee et al. 2018). (If $u(t) < u_{\max}$, we can always increase $E(T)$ by converting at $u_{\max}$ at any time t and still continue to grow the RB population.) For this range of $u_{\max}$, taken in the form

$$u_\alpha \equiv u_{\max} - \alpha > 0, \tag{37}$$

we first observe the following properties for the solution of the problem:

Property 1: For $u_\alpha > 0$, we must have

$$(i)\ \ u_{op}(t) = u_{\max}, \quad (ii)\ \ \lambda(t) < 1, \tag{38}$$

in some interval $t_s < t \leq T$ for some $t_s < T$.

Since $R(t) > 0$ for all t in $[0, T]$, we must convert at $u_{\max}$ at the terminal time; otherwise we can always increase $E(T)$ by converting at a higher rate. The optimal control (38) follows from continuity of state and adjoint functions (given $u(t)$ is PWS), proving part (i).

Upon observing (i), the Hamiltonian (30) becomes

$$[H] = u_{\max} R(t)\,[1 - \lambda(t)] + \alpha\,[\lambda(t) R(t)]\,, \qquad (t_s < t \leq T)$$

requiring $\lambda(t) < 1$ for t in the interval $(t_s, T]$ adjacent to the terminal time T (for the Hamiltonian would not be maximized by $u_{\max}$ in that interval otherwise) proving part $ii)$. (The property can also be proved by invoking the Euler boundary condition (32).)

Property 2: If $(t_s, T]$ is the largest interval adjacent to T in which (38) holds for $u_\alpha > 0$ and $0 < t_s < T$, then t_s must be the zero of $\lambda(t) = 1$ nearest to T, giving us the *switch condition*

$$\lambda(t_s) = 1, \tag{39}$$

for determining the *switch point* t_s of the optimal control $u_{op}(t)$.

Property 3: In the interval $(t_s, T]$ where the Hamiltonian is maximized by $u_{\max}$ (with $\lambda\,(t) < 1$ for $u_\alpha > 0$), the adjoint DE (31) for $\lambda(t)$ simplifies to

$$\lambda' = u_\alpha \lambda - u_{\max}. \tag{40}$$

It follows that $\lambda(t)$ *is monotone decreasing with (increasing) time* in $(t_s, T]$ given $\lambda(t) < 1$ in that interval.

Remark 3 The property is also a consequence of the exact solution

$$\lambda(t) = c_0 e^{u_\alpha (t-T)} + \frac{u_{\max}}{u_\alpha} \qquad (t_s < t \leq T) \tag{41}$$

for the terminal value problem defined by (40) and (32) where the constant of integration c_0 is determined by the Euler boundary condition to give

$$\lambda(t) = \frac{u_{\max}}{u_\alpha} \left(1 - e^{u_\alpha (t-T)}\right) \qquad (t_s < t \leq T). \tag{42}$$

Property 4: With $\lambda(t)$ increasing as t decreases, there exists an instant $t_s < T$ when (39) holds. The "switch condition" (39) determines the switch point t_s to be

$$e^{u_\alpha (t_s - T)} = \frac{\alpha}{u_{\max}}, \quad \text{or} \quad t_s = T - \frac{1}{u_\alpha} \ln\left(\frac{u_{\max}}{\alpha}\right) < T \tag{43}$$

given $0 < \alpha < u_{\max}$. Hence, the switch point occurs prior to the terminal time (though both are still unknown prior to the application of the threshold condition (28)).

We are now in a position to state the following key result for our optimal control problem:

Proposition 4 *The optimal conversion strategy for* $u_{\max} > \alpha$ *is*

$$u_{op}(t) = \begin{cases} 0 & [0 < t < t_s) \\ u_{\max} & (t_s < t \le T] \end{cases}, \tag{44}$$

where the switch point t_s *is determined by* (43)*. (Note that* $t_s \downarrow 0$ *as* $u_{\max} \downarrow \alpha$*.)*

Remark 4 The relative simple proof of this proposition is given in "Appendix B". When $u_{\max} \gg \alpha$, it would seem advantageous not to convert immediately near the start and allow the RB population to grow initially for a while. The larger RB population at a later time would then be converted at the fastest pace possible leading to a larger terminal EB population. Proposition 4 not only succinctly captures the essence of this advantageous strategy, it also provides the indispensable specification of the most opportune time to start converting for maximal spread of infection.

A conversion strategy of the form (44) involving two distinct strategies with a finite jump discontinuity at the instant when a switch from one strategy to the other is known as a *bang-bang control* in the control literature (Bryson and Ho 1969; Wan 1995).

3.6 Terminal Time

With the optimal bang-bang control (44), it is straight forward to use the growth dynamics (25) and (26) to determine the corresponding $R(t)$ and $E(t)$ to be

$$R_{op}(t) = \begin{cases} Ne^{\alpha t} & (0 \le t \le t_s) \\ Ne^{\alpha t_s} e^{-u_\alpha (t-t_s)} & (t_s \le t \le T) \end{cases},$$

and

$$E_{op}(t) = \begin{cases} 0 & (0 \le t \le t_s) \\ \frac{u_{\max}}{u_\alpha} Ne^{\alpha t_s} \left[1 - e^{-u_\alpha (t-t_s)}\right] & (t_s \le t \le T) \end{cases}.$$

The lysis condition (28) then gives the following requirement relating the terminal time T and the switch point t_s:

$$e^{-u_\alpha (T-t_s)} = \frac{p_c e^{-\alpha t_s} - \gamma}{m_c - \gamma}, \qquad \gamma = \frac{u_{\max}}{u_\alpha}, \qquad p_c = \frac{P_c}{N}. \tag{45}$$

This relation and the switch condition (43) determine the optimal switch point t_s and terminal time T. The solution

$$t_s = \frac{1}{\alpha} \ln \left(\frac{p_c}{1 + m_c \alpha / u_{\max}} \right) \tag{46}$$

shows the switch point t_s to be always positive (since we have typically $p_c = P_c/N \gg m_c + 1 > 1 + \alpha m_c / u_{\max}$) and a monotone increasing function of p_c with

$$\frac{p_c}{m_c + 1} = \left[e^{\alpha t_s}\right]_{u_{\max} = \alpha} \le e^{\alpha t_s} < \left[e^{\alpha t_s}\right]_{u_{\max} \to \infty} = t_s.$$

The optimal terminal time T_{op} may be written as

$$\begin{aligned}\alpha T_{op} &\equiv [\alpha T]_{u=u_{op}(t)} = \alpha t_s + \frac{\alpha}{u_\alpha} \ln\left(\frac{u_{\max}}{\alpha}\right) \\ &= \ln\left(\frac{p_c}{1 + m_c \alpha / u_{\max}}\right) + \frac{\alpha}{u_\alpha} \ln\left(\frac{u_{\max}}{\alpha}\right), \end{aligned} \tag{47}$$

With $p_c = P_x/N \gg 1$, we have generally

$$\alpha T_{op} = O\left(\ln\left(\frac{P_c}{N}\right)\right).$$

Proposition 5 *For the biologically relevant case of $u_\alpha > 0$, the optimal host cell lysis time of the WS-Model for maximum expected terminal EB population is of the order of $ln(p_c)$ and is an decreasing function of the weight factor m_c (which may be negative when the inhibiting effect of RB dominates).*

Thus. the time to the optimal expected terminal EB population is an order of magnitude maller than $\alpha T_{op} = O(p_c)$ for $u(t) = \alpha\ (= \lambda_D)$ [see (24)] when λ_C is time invariant.

4 Uncertain Host Death (*The RT-Model*)

4.1 Terminal Time as a Random Variable

Chlamydia species differ in the length of their developmental cycle, e.g. C. trachomatis takes about 48 h whle C. pneumoniae takes about 72 h (Elwell et al. 2016; Hybiske and Stephens 2007). But for a given species, host cell lysis occurs within a relatively narrow time window. Yet it is also true that the range of time of host cell lysis hasn't been well quantified. In the absence of definitive knowledge of the cause or process that induces host cell lysis, we formulated in the last section a plausible model, the *WS-Model*, that provides a criterion for terminating the Chlamydia developmental cycle. To the extent that there is no conclusive evidence to validate (or refute) the criterion, we offer here another plausible approach to the determination of the termination time of a life cycle. In the present approach, we take the lysis times of different infected host cells to be random events induced by the different random embedding environments of the infected cells. The evolution of the two Chlamydia populations are the stochastic processes associated with the stochasticity for which data are available for the uncertain terminal time T. As such T may be taken as a random variable with a prescribed *probability density function* (pdf) $p_T(t)$ (to be estimated from the data available) and the stochastic processes of evolving RB and EB populations induced be characterized by the birth and death processes governed by (1) and (2),

For the purpose of analysis, we take the initial time $t = 0$ to be the instant a group of endocytosed infecting EB transforming into RB units that are positioned to grow and divide. Since host cells are known not to lyse before some $T_1 > 0$ (e.g., 40 hpi

$< T_1 < 48$ hpi), we should let

$$p_T(t) = U(t - T_1) f_T(t) = \begin{cases} 0 & (t < T_1) \\ f_T(t) & (t > T_1) \end{cases}$$

where $f_T(t)$ is the non-zero part of $p_T(t)$ with

$$\int_{-\infty}^{\infty} p_T(\tau)\mathrm{d}\tau = \int_{T_1}^{\infty} f_T(\tau)\mathrm{d}\tau = 1.$$

where $U(z)$ is the Heaviside unit step function with a unit jump at $z = 0$.

The corresponding EB population at the terminal time is also a random variable $E(T)$, a transformed random variable of the random variable T. The *expected value* of $E(T)$, denoted by E_T, is given in terms of the pdf $p_T(\tau)$ by

$$E_T = \int_{-\infty}^{\infty} E(\tau) p_T(\tau)\mathrm{d}\tau = \int_{T_1}^{\infty} E(\tau) f_T(\tau)\mathrm{d}\tau.$$

For simplicity, we continue to work with the two-form *Chlamydia* model of Sect. 3 so that we have from the growth dynamics (25) of EB

$$E(T) = \int_0^T u(t) R(t)\mathrm{d}t.$$

For maximum spread of the C. trachomatis bacteria, we choose the (per unit RB particle) conversion rate $u(t)$ to maximize the expected terminal *EB* population E_T:

$$E_T = \int_{T_1}^{\infty} f_T(\tau) \left[\int_0^{\tau} u(t) R(t)\mathrm{d}t \right] \mathrm{d}\tau. \tag{48}$$

subject to the conversion capacity inequality constraint (29). Upon interchanging the order of integration, we may re-write the expression above as

$$E_T = \int_0^{\infty} F_c(\tau) u(\tau) R(\tau)\mathrm{d}\tau \tag{49}$$

where

$$F_c(t) = \begin{cases} \int_t^{\infty} f_T(\tau)\mathrm{d}\tau & (t \geq T_1) \\ 1 & (t \leq T_1) \end{cases} \tag{50}$$

is the probability of the host cell NOT lysed at time t.

Given the empirical data reported in Lee et al. (2018) showing all host cells to have lysed by 72 hpi. all pdf should be with compact support, so that

$$p_T(t) = U(t - T_1) U(T_2 - t) f_T(t) \tag{51}$$

and

$$F_c(t) = \begin{cases} 0 & (t \geq T_2) \\ \int_t^{T_2} f_T(\tau)\mathrm{d}\tau & (t_1 \leq t \leq T_2) \\ 1 & (t \leq T_1) \end{cases} \tag{52}$$

Typical probability density functions include the *uniform density distribution (over the interval* (T_1, T_2)*)*

$$p_T(t) = \frac{1}{\Delta}\left[1 - U(t - T_2)\right] U(t - T_1), \qquad \Delta = T_2 - T_1 > 0, \tag{53}$$

and the *generalized inverse distribution density function*

$$p_T(t) = \frac{T_1 T_2}{t^2 \Delta} U(t - T_1) U((T_2 - t). \tag{54}$$

The two corresponding $F_c(t)$ are

$$F_c(t) = \begin{cases} 0 & (t \geq T_2) \\ \frac{1}{\Delta}(T_2 - t) & (T_1 \leq t \leq T_2) \\ 1 & (t \leq T_1) \end{cases} \tag{55}$$

and

$$F_c(t) = \begin{cases} 1 & (t \leq T_1) \\ \frac{T_1}{t\Delta}(T_2 - t) & (T_1 \leq t \leq T_2) \\ 0 & (t \geq T_2) \end{cases}, \tag{56}$$

respectively.

Note that the expected host cell lysis time is given by

$$\bar{T} = \int_{-\infty}^{\infty} t p_T(t)\mathrm{d}t = \int_{T_1}^{T_2} t f_T(t)\mathrm{d}t$$

independent of the growth dynamics or the optimal conversion strategy. For the two particular pdf above, we have

$$\bar{T} = \int_{T_1}^{T_2} \frac{1}{\Delta}\mathrm{d}t = \frac{1}{2}(T_2 + T_1) \qquad \text{(uniform distribution)}$$

and

$$\bar{T} = \int_{T_1}^{T_2} \frac{T_1 T_2}{t\Delta}\mathrm{d}t = \frac{T_2 T_1}{\Delta} \ln\left(\frac{T_2}{T_1}\right) \qquad \text{(generalized inverse distribution).}$$

4.2 A Stochastic Optimal Control Problem

With (49), the optimization of expected terminal EB population takes the form

$$\max_{u \in \Omega} \left\{ E_T = \int_0^{T_2} F_c(t) u(t) R(t) \mathrm{d}t \right\} \tag{57}$$

subject to the IVP (25) and the constraints (29) with Ω being the set of admissible (PWS) controls as previously defined.

To apply the method of optimal control, we introduce the Hamiltonian

$$\begin{aligned} H_s(t) &= u(t)R(t)F_c(t) + \lambda(t)R(t)\{\alpha - u(t)\} \\ &= u(t)R(t)\{F_c(t) - \lambda(t)\} + \alpha\lambda(t)R(t) \end{aligned} \tag{58}$$

with the new Hamiltonian H_s in (58) reduced to the Hamiltonian H for a known T, i.e., $f_T(t) = \delta(t-T)$ where $\delta(x)$ is the Dirac delta function. The Maximum Principle has as a necessary condition for optimality the *adjoint function* (aka *Lagrange multiplier*) $\lambda(t)$ satisfying the adjoint ODE

$$\lambda' = (u - \alpha)\lambda - uF_c \tag{59}$$

for t in the interval $(0, T_2)$, and an associated adjoint (Euler) boundary condition (BC) at T_2

$$\lambda(T_2) = 0. \tag{60}$$

The Maximum Principle also requires that we choose an admissible u to maximize H_s (Bryson and Ho 1969; Pontryagin 1962; Wan 2018):

$$\begin{aligned} \max_{u \in \Omega}\{H_s[u]\} &= \max_{u \in \Omega} R^*(t)[u(t)\left\{F_c(t) - \lambda^*(t)\right\} + \alpha\lambda^*(t)] \\ &= H_s[u_{op}(t)], \end{aligned} \tag{61}$$

subject to the inequality constraints

$$0 \le u \le u_{\max}$$

with $(\ )^* = (\ )_{u=u_{op}(t)}$. Since the Hamiltonian is linear in the control function $u(t)$, the optimal control is expected to be a combination of *singular controls* and *extreme values* of the admissible control over different time intervals.

4.3 Singular Solution Not Applicable

Candidates for the maximizers of H_s are normally among the stationary points of the Hamiltonian, i.e., the solutions of

$$\frac{\partial H_s}{\partial u} = [R(t)\{F_c(t) - \lambda(t)\}] = 0. \tag{62}$$

With $R(t)$ changing at the rate $(\alpha - u)R \geq (\alpha - u_{\max})R$, the RB population remains positive for all time as long as $N > 0$ so that the stationary condition requires

$$\lambda_S(t) = F_c(t). \tag{63}$$

Note that the control $u(t)$ does not appear in the stationary condition (62) and hence is not determined by (62). As an immediate consequence of the stationary condition (63), the *singular solution* $\lambda_S(t)$ with the corresponding singular control $u_S(t)$ is to be deduced from other requirements of the Maximum Principle as appropriate. For our problem, the adjoint DE requires

$$F_c'(t) = -\alpha F_c(t)$$

which is generally not satisfied by the probability distribution $F_c(t)$ of the host cell not lysing (and certainly not by the two illustrative examples in (55) and (56)). Hence, the singular solution is generally not applicable in any interval of the solution domain $[0, T_2]$ and we have the following negative result for our problem:

Proposition 6 *The singular solution* (63) *is not applicable in any part of the solution domain for our uncertain terminal time problem.*

Remark 5 It follows from Proposition 6 that the optimal control can only be a combination of the two extreme values 0 and $u_{\max}$ of the constraint on $u(t)$ known as the lower and upper corner control, respectively, in the control literature. Similar to the WS Model, we consider here only the biologically relevant range $u_\alpha > 0$ (see Figure 5G of Lee et al. 2018),

$$u_\alpha = u_{\max} - \alpha, \tag{64}$$

4.4 Optimal Conversion for $u_{\max} > \alpha$

With $R(t) > 0$, $u(T_2) < u_{\max}$ is not optimal since we can always choose a larger u (still within the admissible range) to convert some of the remaining RB for a larger EB population at T_2. With $u_{op}(T_2) = u_{\max}$, we have from the adjoint DE

$$\lambda_g'(T_2) = -u_{\max} F_c(T_2) \leq 0 \tag{65}$$

where $\lambda_g(t)$ denotes the adjoint function with $u(t) = u_{\max}$. Along with the continuity of $\lambda(t) - F_c(t)$, the condition (65) requires that $u_{op}(t)$ must be $u_{\max}$ for some interval $(t_s, T_2]$ adjacent to T_2. We state this observation more formally in the following proposition with a formal proof:

Proposition 7 *The upper corner control maximizes the Hamiltonian* (58) *for some interval* $(t_s, T_2]$ *with* t_s *being the largest root of the switch condition (nearest to* T_2*)*

$$S_g(t) \equiv F_c(t) - \lambda_g(t) = 0. \tag{66}$$

Proof see "Appendix C". □

Having Proposition 7, it remains to determine for the $u_\alpha = u_{\max} - \alpha > 0$ range: *i*) the optimal control in the complementary range $[0, t_s)$, *ii*) the switch point t_s; and *iii*) the optimal expected terminal EB population E_T. (Note that the expected terminal time has already been determined from the pdf of T.) For these tasks, we need the adjoint function for the entire solution interval $[0, T_2]$. .

The adjoint function for the upper corner control $u_{\max}$ adjacent to the terminal time, denoted by $\lambda_g(t)$, is determined by the terminal value problem:

$$\lambda_g' = -(\alpha - u_{\max})\lambda_g - u_{\max} F_c(t), \qquad \lambda_g(T_2) = 0. \tag{67}$$

The solution for a finite T_2 and any t in the interval $[0, T_2]$ is

$$\lambda_g(t) = \begin{cases} 0 & (t \geq T_2) \\ \Lambda_2(t) & (T_1 \leq t \leq T_2) \\ \Lambda_1(t) & (t < T_1) \end{cases} \tag{68}$$

where $\Lambda_k(t)$ depends on the specific $F_c(t)$ in the relevant time interval.

For $u_\alpha > 0$, we know from Proposition 7 that the upper corner control $u_{\max}$ is optimal for (t_s, T_2) where t_s is the largest zero of (66). If $u_{\max}$ should also be optimal for $t \lesssim t_s$ for the uniform pdf (53), then the ODE for the adjoint function at t_s (the zero of (66)) simplifies to

$$\lambda_g'(t_s) = -\alpha \lambda_g(t_s) = -\alpha F_c(t_s) < 0$$

since $\lambda_g(t_s) = F_c(t_s)$. With $\lambda_g(t_s)$ an exponentially decreasing function of t for $t \lesssim t_s$ and $F_c(t)$ typically decreases algebraically (as in the two examples (55) and (56)), we have

$$\lambda_g(t) > F_c(t) \text{ for } t \lesssim t_s.$$

contradicting $u_{\max}$ being optimal there. Since the singular control is not applicable, the lower corner control becomes the only option. This leads to the following proposition for the optimal control:

Proposition 8 *For $u_\alpha > 0$, the lower corner control maximizes the Hamiltonian in $[0, t_s)$ so that the optimal control is the bang-bang control*

$$u_{op}(t) = \begin{cases} 0 & [0 < t < t_s) \\ u_{\max} & (t_s < t \leq T_2] \end{cases}, \tag{69}$$

where t_s is given by switch condition

$$\lambda_g(t_s) = F_c(t_s). \tag{70}$$

Proof see "Appendix D". □

5 Uniform Density on a Finite Interval (*The RT-Model*, Continued)

5.1 The Adjoint Function

For the remaining two tasks, determining the switch point t_s; and the optimal expected terminal EB population E_T, we need the functions $\Lambda_k(t)$, $k = 1, 2$. We illustrate the method of the solution by working out in the this section the details for the uniform density function (53). For this pdf, it is straightforward to solve the relevant terminal value problems to get

$$\Lambda_2(t) = \frac{u_{\max}}{u_\alpha^2 \Delta} \left\{ u_\alpha \, (T_2 - t) - \left[1 - e^{-u_\alpha (T_2 - t)} \right] \right\} \tag{71}$$

$$\Lambda_1(t) = \frac{u_{\max}}{u_\alpha^2 \Delta} \left\{ u_\alpha \Delta - \left[e^{-u_\alpha (T_1 - t)} - e^{-u_\alpha (T_2 - t)} \right] \right\} \tag{72}$$

with $\Delta = T_2 - T_1$. Note that $\lambda_g(t)$ is continuous at T_1 and T_2. That $\lambda_g(t) = 0$ for $t \geq T_2$ reflects the fact that the reticulate bodies have no "(shadow) value" beyond T_2. With $F_c(t) = 0$ for $t \geq T_2$, the host cell has already lysed with probability 1 so that we would only be interested in the range of time $t < T_2$.

5.2 The Switch Point t_s

The process of determining the switch point t_s for $u_{\max} > \alpha$ depends on the location of t_s since the expressions for $F_c(t_s)$ and $\lambda_g(t_s)$ vary with that location [see (68)].

5.2.1 $t_s \leq T_1$

The conditions (68) and (72) requires

$$\frac{u_{\max}}{\alpha u_\alpha \Delta} \left[1 - e^{-u_\alpha \Delta} \right] = e^{u_\alpha (T_1 - t_s)}$$

so that

$$t_s = T_1 - \frac{1}{u_\alpha} \ln \left(\frac{u_{\max}}{\alpha \Delta} \frac{1 - e^{-u_\alpha \Delta}}{u_\alpha} \right). \tag{73}$$

As $u_{\max}$ increases (with α fixed), the switch point t_s tends to T_1 and may have already moved into the $t_s > T_1$ range (to be discussed below). At the other extreme, the switch point t_s in this range tends to 0 (or less) as $u_{\max} \downarrow \alpha$ from above.

5.2.2 $T_1 < t_s \leq T_2$

For t_s in the interval (T_1, T_2), we have from (71) and (68)

$$e^{-x} = 1 - \frac{\alpha}{u_{\max}} x, \qquad x = u_\alpha \, (T_2 - t_s) \tag{74}$$

Unlike the case $t_s \leq T_1$, the switch condition does not determine t_s explicitly. Instead, it only leads to a nonlinear equation for t_s. Graphing the two sides of (74) as functions of x with α and $u_{\max}$ prescribed shows that the switch condition determines a unique positive root x^* with

$$t_s = T_2 - \frac{x^*}{u_\alpha} > T_2 - \frac{u_{\max}}{\alpha u_\alpha}. \tag{75}$$

bounded above by T_2 and below by $T_2 - u_{\max}/(\alpha u_\alpha)$. For a fixed α, we have

$$t_s \to T_2 - 1/\alpha \quad \text{as} \quad u_{\max} \to \infty$$

while t_s should move into the $t_s < T_1$ range as $u_{\max} \downarrow \alpha$.

5.3 The Optimal Expected Terminal EB Population

5.3.1 A Local Maximum

For $u_\alpha > 0$, we know from Proposition 8 that the bang-bang control (69) maximizes the Hamiltonian with t_s determined by (75) or (73) whichever is appropriate. Now maximizing the Hamiltonian is not synonymous with maximizing E_T, we still need to prove that $u_{op}(t)$ maximizes E_T for $u_\alpha > 0$.

Proposition 9 *For $u_\alpha > 0$, the bang-bang control (44) maximizes the expected terminal EB population.*

Proof From Propositions 7 and 8, we know already that $u_{op}(t)$ as given by (44) maximizes the Hamiltonian H_s with t_s in the interval (T_1, T_2). For our relatively simple control problems, we may appeal to the uniqueness of the switch point and that the optimal control is superior to not-converting any RB to EB at all to complete the proof. □

5.3.2 The Expected Terminal EB Population

For the optimal conversion strategy $u_{op}(t)$ given in (44), we have from the growth dynamics (25)

$$R_{op}(t) = \begin{cases} Ne^{\alpha t} & (0 \leq t \leq t_s) \\ Ne^{-u_\alpha t + u_{\max} t_s} & (t_s \leq t < T) \end{cases}. \tag{76}$$

The associated expected EB population is given by (57) so that

$$\begin{aligned} E_T &= \int_0^{T_2} u_{op}(t) F_c(t) R_{op}(t) \mathrm{d}t = u_{\max} N e^{\alpha t_s} \int_{t_s}^{T_2} F_c(t) e^{-u_\alpha (t - t_s)} \mathrm{d}t \\ &= \frac{u_{\max} N e^{\alpha t_s}}{u_\alpha} \begin{cases} E_2(t_s) & (t_s \geq T_1) \\ E_1(t_s) & (t_s \leq T_1) \end{cases} \end{aligned} \tag{77}$$

with

$$E_2(t_s) = \frac{1}{u_\alpha \Delta} \left\{ u_\alpha (T_2 - t_s) - \left[1 - e^{-u_\alpha (T_2 - t_s)} \right] \right\}$$

$$E_1(t_s) = \frac{1}{u_\alpha \Delta}\left\{u_\alpha \Delta\left[2 - e^{-u_\alpha(T_1 - t_s)}\right] - \left[1 - e^{-u_\alpha \Delta}\right]\right\}$$

where $\Delta = T_2 - T_1$ and t_s is determined by (75) if $t_s \geq T_1$ or (73) if $t_s \leq T_1$.

6 A Two-Step Growth and Conversion Model (*the MP-Model*)

6.1 A Conversion Holiday at the Start

That the optimal conversion strategy from our two constrained optimal control models, the *WS-Model* and the *RT-Model*, for maximizing the expected terminal EB population turns out to be a bang-bang control (44) for $\alpha < u_{\max}$ is rather gratifying. Without any presumption of an initial conversion holiday or any enabling mechanism (such as a size-threshold for conversion to ensure its occurrence) the optimal conversion strategy deduced for both models unequivocally anticipates the experimental findings in Lee et al. (2018). If nothing else, they help to buttress our posit that natural selection is at work to result in the observed developmental cycle.

The relevant data (averaged over inclusions) supporting the theoretical optimal conversion strategy summarized in Table 1 have been excerpted from the pie chart of Figure 1 of Lee et al. (2018). The RB unit total reported in this summary includes both (RB and DB) types of this form that were actually reported: those that are ready and eventually convert into EBs and those not ready to convert but ready to divide by binary fission. The conversion of RB is first into *intermediate body*, denoted by IB, that eventually becomes EB with total EB reported in Table 1 here being the sum of both types. The pie-charts in Figure 1 of Lee et al. (2018) show only RB of both types in the infected cells 20 h post infection (hpi). With data collected every 4 hpi, the conversion to IB and then to EB begins sometimes around 24 hpi. This is well after the infecting EB entering the host cell, over a time period nearly half way through the development cycle.

The total EB population (the sum of IB and EB actually observed) rises quickly to 192 units at 28 hpi indicating a maximum possible conversion rate that is much greater than the natural RB proliferation rate. They also show a sharp rise of IBs and EBs at a nearly discontinuous conversion rate around $t_s \lesssim 24$ hpi. Furthermore, with the total RB population declining sharply after reaching a peak of 507 units at 32 hpi, the corresponding gain in EB units becomes slower as shown by the available data up to 40 hpi. These observations provide further support for conversion being proportional

Table 1 Mean count of RB and EB (averaged over inclusions)

Bodies	hpi								
	12	16	20	24	28	32	36	40	> 40
RB	1.3	7.6	34	105	385	507	271	171	Not reported
EB	0	0	0	3.7	192	656	706	751	Not reported

to the RB population size as modeled by (26) and with a conversion rate upper bound $u_{\max} R$ considerably higher than the natural growth rate αR for the RB form.

It would be natural at this point to make use of parameter values (for α, $u_{\max}$, etc.) estimated in Lee et al. (2018) to calculate relevant quantities such as the switch point t_s, terminal time T and other information pertaining to the mean populations of interest. However, the available data from Table 1 excerpted from Lee et al. (2018) suggest that our models still need further refinement before embarking on this task. From the growth dynamics of the RB population modeled by (25), we see for the relevant range $\alpha < u_{\max}$ of interest here that the RB population grows exponentially prior to the onset of conversion (since $u_{op}(t) = 0$ during the conversion holiday at the start) but begins to decline immediately after the switch point t_s ($\simeq$ 24 hpi) since $R' = \alpha - u_{\max} < 0$ (for $t > t_s$). On the other hand, the total RB population reported in Table 1 continues to increase for a period after the appearance of EB particles around 24 hpi. That total only starts to decline after reaching a maximum of 507 units at 32 psi. This important qualitative difference is likely due to the lumped form simplification in the models formulated herein. Without multiple divisions to reach the conversion eligibility threshold size, these two-form models are not sufficiently fine-grained for matching the reported data beyond the conversion holiday phase of the bacterial growth. To remedy this discrepancy, we consider in the next section a four form model, to be known as the *MP-Model*, that allows for two different types each of RB (RB and DB) and EB (IB and EB) as actually recorded in Lee et al. (2018). Such a model was formulated in both Lee et al. (2018) and Wan and Enciso (2017). The additional step of transitioning to another form before division will be shown to rectify the discrepancy in the post conversion holiday RB growth.

6.2 A Multi-form Population Model

In addition to RBs and EBs, intermediates of RB division (known as dividing RB or DB for brevity) and RB-to-EB conversion (known as intermediate body or IB) have been identified and reported separately in Lee et al. (2018) for their distinctive appearance on electron micrographs and shown in Table 2.

A more realistic model for *C. trachomatis* differentiation and proliferation would work with a four-form model as in the schematic diagram of Figure 2 (Wan and Enciso 2017). At any instant of time in this MP-Model, some (eligible) RB units of the population $R(t)$ may convert into an *Intermediate form* $I(t)$ at the rate uR (that would eventually become EB) while the remainder of $R(t)$ to be transitioned into DB form at the rate $\alpha_1 R(t)$. Each unit of the DB population $D(t)$ is capable of binary division into two new RB at the rate $\alpha_2 D$. The population $I(t)$ of Intermediate form converts to EB at a rate bI. The growth rates of the four populations are summarized mathematically by the following four differential equations:

$$R' = -(\alpha_1 + u)R + 2\alpha_2 D, \quad D' = \alpha_1 R - \alpha_2 D, \tag{78}$$

$$I' = uR - bI, \quad E' = bI \tag{79}$$

Table 2 Mean count of RB and EB (averaged over inclusions)

Bodies	hpi								
	12	16	20	24	28	32	36	40	> 40
RB/DB	0.6/0.7	3.9/3.7	17/17	43/52	195/190	263/244	171/100	120/41	Not reported
IB/EB	0	0	0	3.4/0.3	107/85	272/324	192/514	107/644	Not reported

starting with some initial populations

$$R(0) = R_0, \quad D(0) = D_0, \quad I(0) = I_0, \quad E(0) = 0 \tag{80}$$

with DB (the dividing RB) and IB (the intermediate body) populations typically taken to be zero initially so that $D_0 = I_0 = 0$. The MP-Model (78)–(80) was first developed in Wan and Enciso (2017) as a refinement of the PT-Model. It may also be taken as the dynamics for the mean populations of the four stochastic population process in a birth and death model analogous to (1) and (2) for the two-form case.

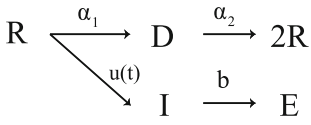

From the second ODE in (79), we get the total EB population at the time of host cell death T

$$E(T) = \int_0^T bI(t)\mathrm{d}t$$

The problem of determining the (PWS) optimal RB-to-EB conversion strategy $u(t)$ (to result in the largest possible (mean) terminal EB population $E(T)$ at the time T when the host cell lyses) takes the form

$$\max_{0 \le u \le u_{\max}} \left[E(T) = \int_0^T bI(t)\mathrm{d}t \right], \tag{81}$$

subject to the growth dynamics of the first three ODE of (78) and (79), the first three initial conditions of (80) and the inequality constraints (29). As a refinement of the WS-Model, some condition for determining the terminal time T would also be prescribed. A parallel development for a refinement of the RT-Model can also be formulated but will not be needed for the present purpose.

6.3 The Post Conversion Holiday RB Population

Given that all population change rates are linear, the optimal control is expected (and can be shown) to be bang-bang for $u_{\max}$ sufficiently large (Wan and Enciso 2017). Prior to the onset of RB-to-EB conversion at t_s, we have $u_{op}(t) = 0$ with the first two ODE in (78) summed to give

$$C'(t) = \alpha_2 D(t), \quad C(0) = N \tag{82}$$

for $C(t) = R(t) + D(t)$ and $R(0) + D(0) \equiv R_0 + D_0 = N$. Since $D(t) > 0$ for $t > 0$, we have $C'(t) > 0$ so that the total RB population increases with time at least up to the onset of the RB-to-EB conversion at time t_s.

For $t > t_s$, we have from the bang-bang control $u_{op}(t) = u_{\max}$ so that

$$C' = -u_{\max} R^{(c)} + \alpha_2 D, \quad C(t_s) = C_s \tag{83}$$

with $C_s = R_s + D_s$ where R_s and D_s are, by continuity of the population sizes, the values of R and D at the switch point t_s determined by the IVP defined by (78) with $u = 0$ and the first two initial conditions in (80). Consistent with the grouping in Lee et al. (2018), the RB population in our four form model consists of two groups: those at or below the critical small size threshold and can convert (to be denoted by $R^{(c)}(t)$) and those (larger than the threshold size,) still growing and not ready to divide. Only the group $R^{(c)}(t)$ can divide; as such, the uR term in the rate of change of R of the MP-Model is an artificial simplification to avoid the complexity of dealing with multiple rounds of division before resulting in a convertible RB and the superscript "(c)" in (83) is to remind us of that fact.

With $C_s = R_s + D_s > 0$ and the various population sizes continuous in time, we have the the following important conclusion for rectifying the noted deficiency pertaining to the post conversion holiday growth of the total RB+DB population:

Proposition 10 *The combined RB+DB population $C(t)$ continues to increase at least for t in some interval (t_s, t^*). The increase continues to a larger interval (t_s, t^{**}) for some $t^{**} > t^*$ if*

$$\alpha_2 D_s > u_{\max} R_s^{(c)}. \tag{84}$$

Proof At $t = t_s$, $C(t)$ is increasing given (82). It continues to increase since $R_s^{(c)}$ is generally small relative to D_s for t_s+ (since those below critical threshold size can convert immediately with finite probability so that the population of that convertible group must necessarily be very small near t_s, assuring the inequality (84) in a small interval (t_s, t^{**}) for some $t^{**} > t^* > t_s$). It follows from (83) that $C'(t) > 0$ in (t_s, t^{**}) and the second half is also proved. □

The condition $\alpha_2 D_s > u_{\max} R_s^{(c)}$ of the proposition is met by the data reported in Lee et al. (2018). Crude estimates using the data presented in Lee et al. (2018) yield the comparisons in Table 3 showing $\alpha_2 D(t) > u_{\max} R^{(c)}(t)$ at least for a small interval post conversion holiday. [Even if there should be some inhibiting mechanism (such as that imparted by RB associated with the parameter i in Eq. (20)) so that $R^{(c)}(t_s)$ is not so small, the recorded data leading to Table 3 may be attributed to the slow ramp up of $u(t)$ toward $u_{\max}$ so that $u(t)R^{(c)}(t)$ remains small in some interval (t_s, t^*) again ensuring (84).]

As a consequence of the proposition above and the validity of (84) in practice, the combined RB+DB population $C(t)$ should continue to increase (at least for an interval of time post-conversion holiday) after the switch point when the RB-to-EB conversion begins. Hence, a glaring qualitative discrepancy between the highly idealized model of the previous section is rectified by the multi-phase life cycle model of this section.

Table 3 Growth rate estimates

$(t_i, t_i + 4)$	(20, 24)	(24, 28)	(28, 32)
$\Delta D/4 \simeq \alpha_2 D(\bar{t}_i)$	8.75	37	13
$\Delta I/4 \simeq u_{\max} R^{(c)}(\bar{t}_i)$	0.85	26	41

7 Summary of Findings and Implications

The comprehensive examination of the chlamydial inclusion by three-dimensional electron microscopy reported in Lee et al. (2018) provided an exceptionally rich trove of data on the unusual Chlamydia developmental cycle distinguished by

(i) the alternative bacterial fate choices for an RB between division into two RBs, or conversion into an EB;
(ii) the existence of a period of no conversion (called a conversion holiday for brevity) in the first half of the developmental cycle;
(iii) a putative small size threshold for RB-to-EB conversion;
(iv) proposed RB size reduction through repeated divisions to reach this conversion threshold size, and
(v) variability among the times for host cell lysing times for releasing EBs to infect other cells.

These unusual features and others prompted us to initiate a theoretical research project to gain some insight to the bacteria's development. We choose to begin with a Birth and Death model in Sect. 2 to characterize the bacteria's life cycle of division and conversion. This provides a gradual transition from our Gamma distribution based probabilistic GD model introduced and discussed in Lee et al. (2018) to the different optimal control models formulated and investigated in this paper. Notice that other approaches are possible and might lead to similar results, such as using a doubly subscripted quantity P_{kj} to describe the state of the system having k RBs and j EBs. We believe our choice of notation P_k and Q_j provides a more natural transition to the mean population sizes of RBs and EBs, respectively.

A four-form mathematical model (the GD-Model for RB, DB, IB and EB) with parameter values estimated from available data (see Table 1 of Lee et al. 2018) shows that these features can be replicated quite faithfully by a relatively simple probabilistic model (see Figure 5g of Lee et al. 2018 for example). In contrast, the goal of the current work is to examine our posit that the developmental cycle maximizes the spread of the bacterial infection (when the host cell lyses and releases the infectious EB form) by showing the theoretical maximizing strategy corresponds qualitatively to the developmental cycle reported in Lee et al. (2018). In a Darwinian world of natural selection, the maximizing strategy would constitute the bacteria's response to the pressure of species survival, the bio-theoretic basis for the Chlamydia developmental cycle.

For a particular infected cell, the deterministic *PT-Model* in Wan and Enciso (2017) is found to support our posit as the optimal *bang-bang control* strategy to maximize in fact specifies a (very unusual) period of no RB-to-EB conversion at the start of the cycle that is qualitatively the same as reported in Lee et al. (2018). A small size threshold for RB-to-EB conversion eligibility observed in Lee et al. (2018) (but not stipulated by any of the optimal control models) is now seen to provide an instrument for a conversion delay. With available data show some variability of the host cell lysis times among the collection of infected cells examined; probabilistic models should be developed to address the observed stochasticity (accompanied by empirical quantification of the

observed variability for C. trachomatis). Two such models (the WS-Model of Sect. 3 and the RT-Model of Sect. 4), both based on the BD-Model of Sect. 2, are shown to also require a conversion holiday at the start for their optimal strategy for maximizing the mean terminal EB population and thus further support our posit on the collection of infected cell data.

To keep the modeling and analysis manageable, the three relevant (PT-, WS- and RT-) models are for two (lumped) forms (RB and EB) of the Chlamydia population (unlike the four-form GD-Model for RB, DB, IB and EB in Lee et al. 2018). Even with parameter values estimated from reported data, these two-form models are not sufficiently fine-grained for matching the reported data beyond the conversion holiday phase of the bacterial growth (so that replicating faithfully the reported data for the development cycle by these lumped form models is not in the cards). In Sect. 6, we noted this deficiency and show that a four-form MP-Model would have continuing growth of RB+DB for a period after the start of RB-to-EB conversion qualitatively consistent with data reported in Lee et al. (2018).

Overall, we have shown that the delay in RB-to-EB conversion (conversion holiday) is a strategy to maximize infectious yield (i.e. terminal EB population) at the end of the developmental cycle. The timing of replication and conversion in each chlamydia is inherently stochastic, and this leads to variability in population sizes but doesn't appear to significantly change the overall dynamics as shown in these models. We have undertaken a number of comparisons between model predictions and available data, both quantitatively and qualitatively in Lee et al. (2018); Wan and Enciso (2017) and herein. For more quantitative agreement between optimal control models and data on other features such as the switch time for the onset of conversion, the effects of threshold size for conversion, etc., we need to refine the models further to allow for more than four forms in order to capture the multiple divisions required to reach the small size conversion eligibility threshold.

Acknowledgements Funding was provided by National Science Foundation (Grant Nos. DMS1763272, DMS1616233) and National Institutes of Health (Grant No. R01 AI151212).

Appendix

A: Summary and Description of the Six Relevant Models

As the present work is the third report of our work to examine the development of C. trachomatis and its bio-theoretic foundation, we summarize below all the models involved in the discussion herein, both new and previously analyzed, and clarify their relation to each other.

- The *GD-Model*: The data of Lee et al. (2018) reveal a complex developmental cycle that features repeated divisions of an RB form of the bacterium and the conversion of RB to the EB form that survives host cell lysis to infect other human cells and spread the bacteria. A probabilistic model with gamma distributions assigned to the elapsed times between different state transitions, known as the GD-Model herein, was formulated in Lee et al. (2018) to show the empirical findings can be

faithfully replicated by a mathematical model based on a few simple theoretical ingredients.

- The *PT-Model:* The GD-Model reproduces the features of the chlamydial development observed but does not provide a bio-theoretic basis for these features. To address the question what role natural selection plays in these features, a deterministic PT-Model for the evolution of the two (lumped) C. trachomatis populations in a cytoplasmic inclusion was formulated in Wan and Enciso (2017) to focus on the alternative cell fate choices of an RB division into two RBs or an RB conversion into an EB. The resulting RB-to-EB conversion strategy that maximizes the EB population at a known terminal time (without any built-in mechanism to induce the observed conversion holiday at the start of the developmental cycle) is qualitatively the same as that found empirically in Lee et al. (2018).
- The *BD-Model*: The variability of the many features of the chlamydial development among the collection of infected cells examined necessitates formulation and analysis of probabilistic models. The alternative choice of division and conversion is captured by a simple birth and death process model (the BD-Model) for the RB and EB populations in Sect. 2. This BD-Model provides a stepping stone to our two approaches to the optimal control problem for our posit that the development cycle is the optimal strategy for maximizing the spread of the bacterial infection.
- The *RT-Model*: With data available for the lysis time of the infected cells examined, one approach is to treat T as a random variable with a probability distribution (or a density function) estimated from the data. This leads to the stochastic optimal control RT-Model of Sect. 4.
- The *WS-Model*: An alternative approach assumes the variability of lysis time among host cells to be a consequence of the uncertain environment experienced by different host cells and the resulting in random elapsed times transitioning from an RBs to two smaller RBs (after a division) or to an EB (through a conversion) captured by the BD-Model. The lysis time for each host cell in this WS-Model is, as seen from Sect. 3, determined by a threshold condition of a weighted sum of terminal RB and EB populations.
- The *MP-Model*: The highly idealized 2-form models are too coarse-grained for matching with available developmental data. A qualitative difference is observed between the theoretical result and the data reported in Lee et al. (2018) on the post conversion holiday growth of the RB population. The discrepancy is removed by a four-form model, the MP-Model of Sect. 6.

B: Method of Characteristics for Generating Functions

The characteristic ODE of the first order PDE for $G(x, \tau)$ are

$$\frac{\mathrm{d}x}{\mathrm{d}\tau} = -\rho + (1+\rho)x - x^2, \qquad \frac{\mathrm{d}G}{\mathrm{d}\tau} = 0.$$

The Riccati equation for $x(\tau)$ can be written as

$$\frac{\mathrm{d}x}{\mathrm{d}\tau} = (1-x)(x-\rho).$$

with $x_p(\tau) = 1$ as a particular solution. The decomposition

$$x(\tau) = 1 + \frac{1}{z(\tau)}$$

transforms the Riccati equation into a linear ODE

$$\frac{\mathrm{d}z}{\mathrm{d}\tau} - (1-\rho)\, z = 1.$$

with an exact solution

$$z(\tau) = e^{-f(\tau)} \left\{ \frac{1}{x_0 - 1} + I(\tau) \right\}$$

where as given in (9)

$$f(\tau) = -\tau + \int_0^\tau \rho(\xi)\mathrm{d}\xi, \qquad I(\tau) = \int_0^\tau e^{f(\zeta)}\mathrm{d}\zeta,$$

and x_0 is a constant of integration. The corresponding solution for $x(\tau)$ is

$$x(\tau) = 1 + \frac{1}{z(\tau)} = 1 + \frac{(x_0 - 1)\, e^{f(\tau)}}{1 + (x_0 - 1)\ I(\tau)} \tag{85}$$

with

$$x(0) = x_0.$$

The solution for the other characteristic ODE is

$$G(x, \tau) = G_0 = x_0^N \tag{86}$$

since there are exactly N RB units initially so that

$$[G(x, \tau)]_{\tau=0} = G(x_0, 0) = \sum_{k=0}^{\infty} P_k(0) x_0^k = x_0^N.$$

To complete the solution, we solve (85) for x_0 in terms of x and τ to get

$$x_0 = 1 + \frac{x - 1}{e^{f(\tau)} - (x-1) I(\tau)} \tag{87}$$

Upon using this expression for x_0 in (86), we obtain

$$G(x,\tau) = x_0^N = \left\{1 + \frac{x-1}{e^{f(\tau)} - (x-1)I(\tau)}\right\}^N. \tag{88}$$

C: Proof of Proposition 4

Proof The optimal control $u_{op}(t)$ must be the lower corner control 0 at least in a small interval $(t_0, t_s]$ adjacent to the switch point. If not and $u_{op}(t) = u_{\max}$ for $0 \le t_0 < t \le t_s$, then

$$\lambda'(t_s) = u_\alpha \lambda(t_s) - u_{\max} = -\alpha < 0$$

so that $\lambda(t)$ is a decreasing function of t in some small neighborhood of t_s. With $1 - \lambda(t) \le 0$ for $t \le t_s$, the upper corner control $u_{\max}$ does not maximize the Hamiltonian at least for t in that neighborhood; hence, $u(t) = u_{\max}$ is not optimal there. Since the singular solution does not apply, we are left with the only option of $u_{op}(t) = 0$ in that neighborhood. In that case, the adjoint DE (31) and the continuity of the adjoint function require

$$\lambda' = -\alpha\lambda. \quad \lambda(t_s) = 1$$

and therewith

$$\lambda(t) = e^{-\alpha(t-t_s)}, \quad (t \le t_s).$$

With this, the Hamiltonian,

$$H(u) = \alpha\lambda(t)R(t) + \left[1 - e^{-\alpha(t-t_s)}\right]u(t)R(t), \quad (t \le t_s), \tag{89}$$

is maximized by the lower corner control $u_{op}(t) = 0$ for all t in the interval $[0, t_s)$. □

D: Proof of Proposition 7

Proof With the Euler BC $\lambda_g(T_2) = 0$, the Hamiltonian reduces to

$$H_s(T_2) = u(T_2)R_g(T_2)F_c(T_2)$$

(i) For the general case with $F_c(T_2) > 0$, $H_s(T_2)$ is maximized by the upper corner control so that $u_{op}(T_2) = u_{\max}$. Given

$$\lambda_g(T_2) = 0, \quad \lambda_g'(T_2) = -u_{\max}F_c(T_2) < 0,$$

we have $\lambda_g(t) \ge 0$ but, by continuity, $\lambda_g(t) < F_c(t)$ for some interval $(t_s, T_2]$ adjacent to T_2. It follows from $R(t) > 0$ that $u_{op}(t) = u_{\max}$ at least in $(t_s, T_2]$ with t_s being the root of (66) nearest to (but still <) T_2.

(ii) For the case $F_c(T_2) = 0$ (and $F_c(t) > 0$ for $t < T_2$), we have

$$\begin{aligned}\left[\left\{\lambda_g - F_c\right\}'\right]_{t=T_2} &= u_\alpha \left[\lambda_g - F_c\right]_{t=T_2} - \alpha F_c(T_2) + f_T(T_2) \\ &= u_\alpha \left\{\lambda_g - F_c\right\}_{t=T_2} + f_T(T_2) \geq u_\alpha \left\{\lambda_g - F_c\right\}_{t=T_2}\end{aligned}$$

so that $\left[F_c(t) - \lambda_g(t)\right]$ is a decreasing function of t but remains > 0 at least in some interval $(t_s, T_2]$. It follows from (61) that we have $u_{op}(t) = u_{\max}$ at least in $(t_s, T_2]$ with t_s being the root of (66) nearest to (but still $<$) T_2.

□

E: Proof of Proposition 8

Proof We have already $u_{op}(t) = u_{\max}$ for $t_s < t \leq T_2$ from Proposition 7 where the *switch point* t_s is the root of (70) nearest to T_2. We also learned from the development prior to this proposition that $u_{op}(t)$ cannot be $u_{\max}$ or the singular solution for $t \lesssim t_s$.

For the lower corner control in that range, the corresponding adjoint function, denoted by $\lambda_\ell(t)$, is determined by

$$\lambda_\ell' = -\alpha\lambda_\ell, \qquad \lambda_\ell(t_s) = F_c(t_s).$$

The exact solution is

$$\lambda_\ell(t) = F_c(t_s)e^{-\alpha(t-t_s)}.$$

(i) For $t_s \leq T_1$, we have $F_c(t) = 1$ and $\lambda_\ell(t) = e^{\alpha(t_s-t)}$ so that $1 - e^{\alpha(t_s-t)} < 0$ for all $t < t_s$ and

$$H_s(t) = u(t)R(t)\left[1 - e^{\alpha(t_s-t)}\right] + \alpha R(t)e^{\alpha(t_s-t)},$$

is maximized by $u_{op}(t) = 0$ there.

(ii) For $t_s > T_1$, $F_c(t)$ decreases only linearly with increasing t while $\lambda_\ell(t)$ decay exponentially with $\lambda_\ell(t_s) = F_c(t_s)$ so that $u_{op}(t) = 0$ is also optimal for $t < t_s$.

□

References

Abdelrahman YM, Belland RJ (2005) The chlamydial developmental cycle. FEMS Microbiol Rev 29:949–959

Batteiger BE, Tan M (2019) Chlamydia trachomatis (trachoma and urogenital infections). In: Bennett JE, Dolin R, Blaser MJ (eds) Mandell, Douglas, and Bennett's principles and practice of infectious diseases. Elsevier, Philadelphia, pp 2301–2319

Belland RJ et al (2003) Genomic transcriptional profiling of the developmental cycle of *Chlamydia trachomatis*. Proc Natl Acad Sci USA 100:8478–8483

Bryson A, Ho YC (1969) Applied optimal control. Ginn and Company, Waltham

Denk W, Horstmann H (2004) Serial block-face scanning electron microscopy to reconstruct three-dimensional tissue nanostructure. PLoS Biol 2:e329

Elwell C, Mirrashidi K, Engel J (2016) Chlamydia cell biology and pathogenesis. Nat Rev Microbiol 14(6):385–400

Hackstadt T, Fischer ER, Scidmore MA, Rockey DD, Heinzen RA (1997) Origins and functions of the chlamydial inclusion. Trends Microbiol 5:288–293

Hybiske K, Stephens RS (2007) Mechanisms of host cell exit by the intracellular bacterium. Chlamydia. Proc Natl Acad Sci USA 104:11430–11435

Lee JK, Enciso GA, Boassa D, Chander CN, Lou TH, Pairawan SS, Guo MC, Wan FYM, Ellisman MH, Sütterlin C, Tan M (2018) Replication-dependent size reduction precedes differentiation in *Chlamydia trachomatis*. Nat Commun. https://doi.org/10.1038/s41467-017-02432-0

Leighton SB (1981) SEM images of block faces, cut by a miniature microtome within the SEM—a technical note. Scan Electron Microsc Pt 2:73–76

Moulder JW (1991) Interaction of chlamydiae and host cells in vitro. Microbiol Rev 55:143–190

Newman L et al (2015) Global estimates of the prevalence and incidence of four curable sexually transmitted infections in 2012 based on systematic review and global reporting. PLoS ONE 10:e0143304

Pontryagin LS et al (1962) The mathematical theory of optimal control processes. Interscience Publishers, New York

Shaw EI et al (2000) Three temporal classes of gene expression during the *Chlamydia trachomatis* developmental cycle. Mol Microbiol 37:913–925

Taylor HR, Burton MJ, Haddad D, West S, Wright H (2014) Trachoma. Lancet 384:2142–2152

Wan FYM (1995) Introduction to the calculus of variations and its applications. Chapman and Hall, New York

Wan FYM (2018) Dynamical system models in the life sciences. World Scientific, Singapore

Wan FYM, Enciso GA (2017) Optimal proliferation and differentiation of *Chlamydia trachomatis*. Stud Appl Math 139(1):129–178. https://doi.org/10.1111/sapm.12175

World Health Organization (2020) Trachoma Fact Sheet. https://www.who.int/news-room/fact-sheets/detail/trachoma